Multi-level Polar Coded Modulation for the Decode-Forward Relay Channel

Heping Wan, and Aria Nosratinia The University of Texas at Dallas, Richardson, TX, USA

Abstract—We investigate the performance of multi-level polar coded modulation in the decode-forward relay channel. We begin by numerically analyzing the rates assigned to polar codes of all levels via chain rule and error exponent. The construction of polar codes follows the 5G standard. A joint decoding based on maximum ratio combining with multistage decoding is proposed for the destination. We simulate the error performance under 16QAM with gray labeling and Ungerboeck's set partitioning. In the half-duplex mode, a gain of 2.5dB is observed compared with the state of the art, consisting of 0.7dB gain due to multistage decoding and 1.8dB gain due to the choice of labeling. In addition, the error performance according to error exponent is compared with the chain rule. A dispersion bound for the decode-forward relaying is calculated.

I. INTRODUCTION

The utility and importance of relaying has been well established for allowing better and more efficient communications in multi-node networks such as Internet of Things and machine-to-machine communications [1]. This argument is even more pronounced in the short-block length regime, where achieving low error rates is more challenging. There exists an extensive literature, e.g. [2]–[7], for implementing coding protocols for the relay channel by using low density parity check (LDPC) codes, convolutional codes and polar codes [8].

Polar codes are part of the 5G standard [9] and are a competitive option for error control, especially in the short-block length. A variation of polar codes [10] has been shown to operate very close to Polyanskiy's dispersion bound [11]. Other advances in this area include belief propagation list decoding [12]. To operate at high spectral efficiency, multi-level polar coded modulation [13] whose component polar codes are constructed based on 5G standard [9] was introduced.

Because of the factors mentioned above, the operation and performance of polar coded modulation in relaying systems is of great interest. Wang [14] demonstrated that polar code achieved the lower bounds of decode-forward and compress-forward relay channels. Blasco-Serrano et al. [5] used nested polar codes for binary symmetric decode-forward and compress-forward relay channels. Madhusudhanan and Nithyanandan [6] showed that polar code outperformed Turbo code in compress-forward relaying under 16QAM. Ma et al. [7] studied multi-level polar coded modulation in the half-duplex decode-forward relaying with orthogonal receivers.

In this paper, we analyze, design, and simulate multilevel polar coded modulation as a convenient and flexible

This work was made possible in part by the grant 1711689 from the National Science Foundation.

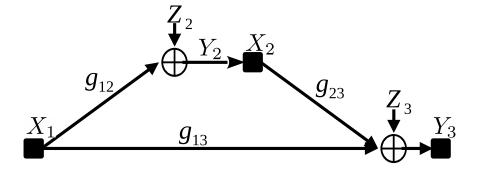


Fig. 1. The relay channel model

method for the implementation of coded modulation in the full-duplex decode-forward relaying in the presence of additive white Gaussian noise (AWGN). In order to compare with the existing literature, we also implement a half-duplex version of our method. We numerically analyze the proper assignment of rates to the component polar codes via chain rule and error exponent. We send the message recovered at the relay, which requires a joint decoding at the destination, instead of sending the binning of the recovered message. A joint decoding algorithm base on maximum ratio combining and multistage decoding is proposed. We design the component polar codes according to 5G standard [9]. 16QAM with gray labeling and Ungerboeck's set partitioning is considered. In the half-duplex mode, a gain of 2.5dB is observed compared with the state of the art [7]; 0.7dB gain is attributed to multistage decoding and 1.8dB gain to the choice of labeling. In addition, the error performance according to error exponent is compared with the chain rule. A dispersion bound for the decode-forward relaying is calculated.

The remainder of this paper is organized as follows. In Section II, the relay channel model, polar code and multilevel polar coded modulation are described. Section III details the rate allocations via chain rule and error exponent, the calculation of dispersion bound as well as the design of multilevel polar coded modulation. In Section IV, simulation results are presented and discussed. Section V concludes the paper.

II. PRELIMINARIES

In this paper, random values are represented with upper-case letters, e.g. Y_2 , deterministic values with lower case letters, e.g. y_2 , and corresponding vectors with bold font, e.g., Y_2 , y_2 .

In our full-duplex relay model, following [2], self-interference is modeled as AWGN, and is absorbed together with the channel noise. The three-node AWGN full-duplex relay channel is shown in Fig. 1. The source and the relay, respectively, have signals X_1 , X_2 with average power constraints P_s , P_r . The AWGN, unit-variance receiver noise at

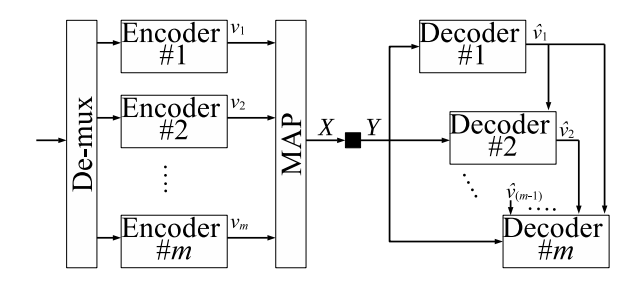


Fig. 2. Multi-level coding with multistage decoding in P2P channel.

the relay and the destination are denoted Z_2, Z_3 . The three channel coefficients g_{13} , g_{12} and g_{23} are known by all three nodes. The received signals are:

$$Y_2 = g_{12}X_1 + Z_2, (1)$$

$$Y_3 = g_{13}X_1 + g_{23}X_2 + Z_3. (2)$$

Full-duplex relaying is implemented by a block-Markov strategy as follows. A sequence of b-1 messages $\{d_j\}_1^{b-1}$ is transmitted over b transmission blocks. Each block has N transmissions. By convention $d_0 = d_b = 1$.

A. Polar Coding

Polar codes are defined with a generator matrix $G_2^{\otimes n}$, where \otimes is the Kronecker product and $G_2 \triangleq \begin{bmatrix} 1 & 0 \\ 1 & 1 \end{bmatrix}$. $U \triangleq [U_1, \cdots, U_N]$ denotes the data to be encoded, where $N = 2^n$. The codeword is denoted with $\mathbf{x} = \mathbf{u}G_2^{\otimes n}$. The i.i.d. channel can be envisioned as N independent copies of a binary discrete memoryless channel (DMC) $W: X \to Y$. Then, individual bit U_i sees a virtual channel $W^{(i)}: U_i \to \{Y, U_1, \cdots, U_{i-1}\}$. As n goes to infinity, the virtual channels are polarized, which means they become either a good (noiseless) channel or a bad (pure-noise) channel. The fraction of good channels is close to the symmetric capacity of W.

We denote with \mathcal{G} the set of indices for the reliable virtual channels. Following Arikan [8], we call \mathcal{G} the *information set* and its complement \mathcal{G}^c the *frozen set*. The data bits corresponding to information set are carried by $\{U_\ell : \ell \in \mathcal{G}\}$ and the bits corresponding to frozen set are fixed and revealed to the destination. Using knowledge of frozen bits $\{u_\ell : \ell \in \mathcal{G}^c\}$, the destination recovers an estimated \hat{u} by using successive cancellation decoding.

B. Multi-level Polar Coded Modulation

Consider a DMC $W: X \to Y$ with input alphabet of size 2^m , m > 1. Multi-level coding (see Fig. 2) is implemented by splitting the data into m binary sub-streams. Each sub-stream is protected independently by a binary error-control code. At each time instance, the output bits of encoders are combined into a labeling vector $\mathbf{v} \triangleq [v_1, \cdots v_m]$ which is mapped to the transmit signal x via a (bijective) mapping. Then, the mutual information between the channel input and output is shown as

$$I(X;Y) \stackrel{(a)}{=} I(V;Y) \stackrel{(b)}{=} \sum_{k=1}^{m} I(V_k;Y|V_1,\cdots,V_{k-1}),$$
 (3)

where V_0 represents a constant, (a) follows the bijective nature of mapping to modulation symbols, and (b) is due to the chain rule of mutual information. Successive decoding is then made possible in the sub-channels implied by Eq. (3), namely $W_k: V_k \to \{Y, V_1, \cdots, V_{k-1}\}$. At each level k, the multi-stage decoder employs the channel observation y as well as the decoded values from preceding levels. To ensure that decoding at each level is reliable, the code rate at level k is chosen to be less than $I(V_k; Y|V_1, \cdots, V_{k-1})$.

Let $U_k \triangleq [U_{k,1}, \cdots, U_{k,N}]$ and $V_k \triangleq [V_{k,1}, \cdots, V_{k,N}]$ denote binary sequences corresponding to level k. In multilevel polar coded modulation, polarization of sub-channels W_k via $v_k = u_k G_2^{\otimes n}$ generates mN virtual sub-channels denoted $W_{k,i}: U_{k,i} \rightarrow \{Y, U_1 \cdots U_{k-1}, U_{k,1}, \cdots, U_{k,i-1}\}$. The rates of component polar codes follow the chain rule (3). Monte Carlo method or density evolution with/without Gaussian approximation [13] can be used to determine corresponding information sets and frozen sets. Knowing frozen bits and recovered codewords of preceding levels, a successive cancellation decoder generates an estimated \hat{u}_k .

III. DECODE-FORWARD

A. Rate-Allocation via Chain Rule

The relay decodes the transmitted message upon receiving y_2 , and helps the source by retransmitting the decoded message in the next block. The achievable rate is given by [15]

$$R_{DF} \le \max_{p(x_1, x_2)} \min\{I(X_1; Y_2 | X_2), I(X_1, X_2; Y_3)\}. \tag{4}$$

In the following, we express this rate in the context of multilevel coding. The source transmit signal X_1 has a bijective mapping with a binary vector $[A_1,...,A_m]$, and the relay transmit signal X_2 has a bijective mapping with a binary vector $[B_1,...,B_m]$. In our strategy, the relay sends the entire recovered message instead of its binning. In this case, the relay may have the rate of codebook above the capacity of the relay-destination link. However, the destination is still able to decode relay signals jointly together with the source signals. For ease of exposition we consider that the multi-level coding at the source and the relay has the same levels; however, this is easily extended to different modulations by forcing certain levels filled with constant [2]. Applying multi-level coding at the source and the relay enables the achievable rate (4) to be further expressed as

$$R_{DF} \le \max \min \left\{ \sum_{k=1}^{m} I(A_k; Y_2 | \mathbf{B}, A_1, \cdots, A_{k-1}), \\ \sum_{k=1}^{m} I(A_k, B_k; Y_3 | A_1, \cdots, A_{k-1}, B_1, \cdots, B_{k-1}) \right\},$$
 (5)

maximized over $\prod_{k=1}^{m} p(a_k|b_k)p(b_k)$. The framework where the source signal of each level only depends on the relay signal at the same level leads to small rate loss [2]. The achievable rates of sub-channels resulting from multi-level coding satisfy

$$R_{DF}(k) \leq \max \min\{I(A_k; Y_2 | \boldsymbol{B}, A_1 \cdots A_{k-1}),$$

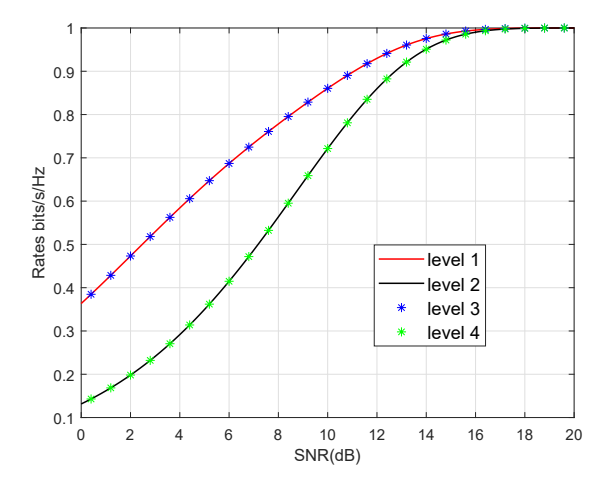


Fig. 3. Rate allocation based on chain rule and 16QAM with gray labeling.

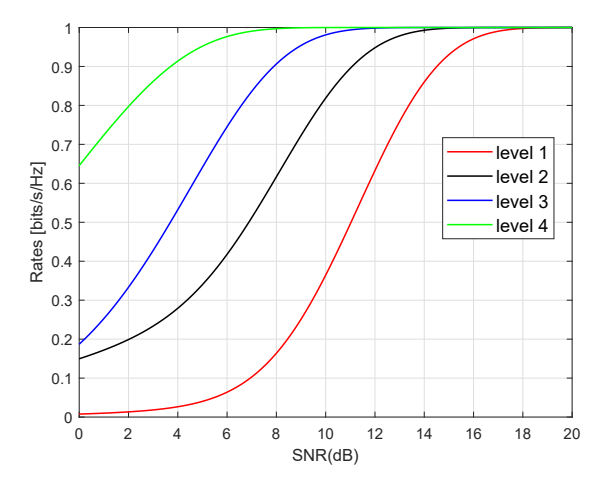


Fig. 4. Rate allocation based on chain rule and 16QAM with Ungerboeck's set partitioning.

$$I(A_k, B_k; Y_3 | A_1, \cdots, A_{k-1}, B_1, \cdots, B_{k-1})$$
. (6)

Figs. 3 and 4 show the chain-rule based rates of all levels using gray labeling and Ungerboeck's set partitioning [16] respectively, where $g_{13} = g_{12} = g_{23} = 1$, $P_s = P_r$ and signal to noise ratio (SNR) corresponds to the source-destination link.

Remark 1. Our encoder at the source generates codewords that depend only on the present message, while the full block-Markov encoding source has codevectors that depend on both the present and past message. This simplification is equivalent to calculating the achievable rates over the set of distributions $p(x_1)p(x_2)$ instead of $p(x_1,x_2)$. This was done in the interest of simplicity of code design as well as avoiding complications in decoding.

B. Rate-Allocation via Error Exponent

1) Error Exponent in P2P Channel: For a P2P channel with multi-level coding in Section II-B, the error exponent $E^k(\mathbb{R}^k)$

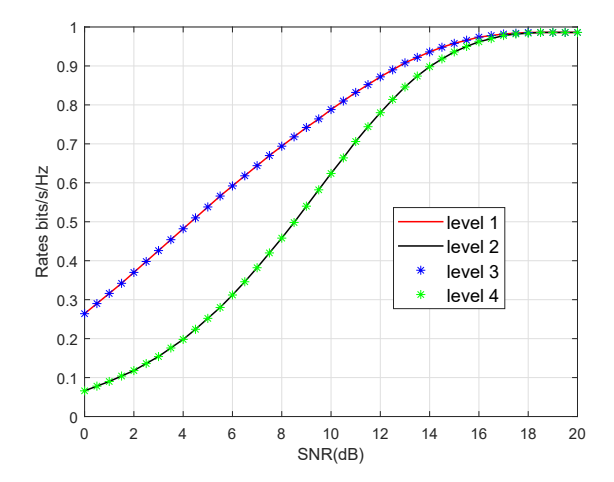


Fig. 5. Rate allocation for N = 256 and $\epsilon^k = 10^{-4}$, k = 1, 2, 3, 4 based on error exponent and 16QAM with gray labeling.

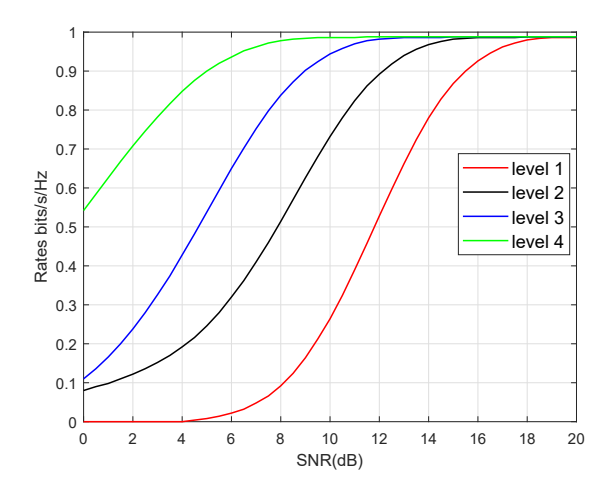


Fig. 6. Rate allocation for N = 256 and $\epsilon^k = 10^{-4}$, k = 1, 2, 3, 4 based on error exponent and 16QAM with Ungerboeck's set partitioning.

of sub-channel W_k with rate R^k is [17]

$$E^{k}(R^{k}) = \max_{0 < \rho < 1} \{ E_{0}^{k}(\rho) - \rho R^{k} \}, \tag{7}$$

where

$$E_0^k(\rho) = \mathbb{E}_{v_1^{k-1}} \left\{ E_0^k(\rho, v_1^{k-1}) \right\}. \tag{8}$$

 v_1^{k-1} in Eq. (8) is defined as a vector $[v_1, \cdots, v_{k-1}]$. Using the error exponent, frame error rate (FER) P_e^k at level k is upper bounded by

$$P_e^k \le 2^{-NE^k(R^k)}. (9)$$

 $E_0^k(\rho, v_1^{k-1})$ in Equation (8) is given by

$$E_0^k(\rho, v_1^{k-1}) = -\log_2 \left\{ \int_Y \left[\sum_{v_k=0}^1 p(v_0) p(y|v_k, v_1, \cdots, v_{k-1})^{\frac{1}{1+\rho}} \right]^{1+\rho} dy \right\}.$$
(10)

Fixing FER to a constant, there is a tradeoff between rates and SNRs.

2) Error Exponent in Decode-Forward: Let $y_2^{(j)}$, $y_3^{(j)}$ and $x_1(d_j)$, $x_2(\tilde{d}_{j-1})$ denote the received and the transmit signals in block j, where \tilde{d}_{j-1} is the estimated message at the relay.

Our work considers that the source and the relay have the same component polar codes and modulations. In this case, the decode-forward relaying is equivalent to a single-input double-output system. Then, we apply maximum ratio combining on the received signals

$$\mathbf{y}_{3}^{(j)} = g_{13}\mathbf{x}_{1}(d_{j}) + g_{23}\mathbf{x}_{2}(\tilde{d}_{j-1}) + \mathbf{z}_{3},$$
(11)
$$\bar{\mathbf{y}}_{3}^{(j+1)} = \mathbf{y}_{3}^{(j+1)} - g_{13}\mathbf{x}_{1}(d_{j+1}),$$
$$= g_{23}\mathbf{x}_{2}(\tilde{d}_{j}) + \mathbf{z}_{3},$$
(12)

with the assumption that $x_1(d_{j+1})$ has been recovered during the backward decoding, or similarly on the received signals

$$\check{\mathbf{y}}_{3}^{(j)} = \mathbf{y}_{3}^{(j)} - g_{23}\mathbf{x}_{2}(\tilde{d}_{j-1}),
= g_{13}\mathbf{x}_{1}(d_{i}) + z_{3},$$
(13)

$$\mathbf{y}_{3}^{(j+1)} = g_{23}\mathbf{x}_{2}(\tilde{d}_{j}) + g_{13}\mathbf{x}_{1}(d_{j+1}) + \mathbf{z}_{3},\tag{14}$$

with the assumption that $x_2(\tilde{d}_{j-1})$ has been recovered during the forward decoding. Thus, the achievable rate (4) is simplified to

$$R_{DF} \le \min \left\{ C(g_{12}^2 P_s), C(S) \right\},$$
 (15)

where $S = \frac{g_{13}^2 P_s}{g_{23}^2 P_{r+1}} + g_{23}^2 P_r$ and $g_{13}^2 P_s + \frac{g_{23}^2 P_r}{g_{13}^2 P_s + 1}$ for respective backward and forward decoding, and $C(x) = \log_2(1+x)$. The first and second term in (15) guarantees the correct decoding at the relay and the destination respectively.

Let the error exponents for the relay and the destination at level k denoted with $E_R^k(R_{CF}(k))$ and $E_D^k(R_{CF}(k))$ respectively which can be calculated via Equations (7), (8) and (10). Thus, the decoding FERs at the relay and the destination denoted ϵ_R^k and ϵ_D^k respectively are related to $E_R^k(R_{CF}(k))$ and $E_D^k(R_{CF}(k))$ in the form of Inequality (9).

The overall FER ϵ^k is bounded by [18]

$$2\epsilon_*^k - \left(\epsilon_*^k\right)^2 \ge \epsilon^k \ge \epsilon_*^k,\tag{16}$$

where ϵ_*^k equals to ϵ_D^k if $g_{12}^2P_s \geq S$ or ϵ_R^k otherwise. Solving Inequalities (16) for a fixed ϵ^k results in a lower bound denoted $L(\epsilon^k)$ of ϵ_*^k . Therefore, $L(\epsilon^k) \leq \epsilon_*^k \leq 2^{-NE_*^k(R_{CF}(k))}$, where $E_*^k(R_{CF}(k)) = E_D^k(R_{CF}(k))$ or $E_R^k(R_{CF}(k))$. Based on the isoquants [17] of the error exponent, $E_*^k(R_{CF}(k)) = -\frac{1}{N}\log_2\left(L(\epsilon^k)\right)$. Thus, fixing ϵ^k enables a tradeoff between $R_{CF}(k)$ and SNRs.

Figs. 5 and 6 show the error-exponent based rates of all levels using gray labeling and Ungerboeck's set partitioning respectively, where $g_{13} = g_{12} = g_{23} = 1$ and $P_s = P_r$.

C. Dispersion Bound

Polyanskiy [11] derived the decoding FER denoted P_e for the point-to-point AWGN channel as a function of block length N and code rate R which was given by

$$P_e = Q\left(\frac{C - R + O(\frac{\log_2(N)}{N})}{\sqrt{\frac{V}{N}\log_2(e)}}\right),\tag{17}$$

where the function $Q(\tau) = \int_{\tau}^{\infty} \frac{1}{\sqrt{2\pi}} e^{-\frac{x^2}{2}} dx$. C, \mathcal{V} respectively denote the achievable rate and dispersion of the channel with constrained input. Denoting Z the unit-variance AWGN and $\{x_i\}$ the set of constellation points with size 2^m , we have [19]:

$$C = m - \frac{1}{2^m} \sum_{i=1}^{2^m} \mathbb{E} \left[\log_2 \left(\sum_{i=1}^{2^m} e^{\|Z\|^2 - \|x_i + Z - x_j\|^2} \right) \right], \quad (18)$$

$$\mathcal{V} = \frac{1}{2^m} \sum_{i=1}^{2^m} \text{Var} \left[\log_2 \left(\sum_{j=1}^{2^m} e^{\|Z\|^2 - \|x_i + Z - x_j\|^2} \right) \right].$$
 (19)

Let ϵ_R and ϵ_D denote FERs at the relay and the destination respectively. Having a modified power constraint $g_{12}^2 P_s$ or S in (15), we can calculate ϵ_R and ϵ_D based on Equations (17)-(19), and therefore the overall FER $\epsilon \approx \epsilon_R + (1 - \epsilon_R)\epsilon_D$.

D. Design of Multi-level Polar Coded Modulation

Let Q_k denote the information set used by both source and relay at level k, and $\frac{|Q_k|}{N} = R_{CF}(k)$. Let $y_{mrc}^{(j)}$ denote the maximum ratio combining of (11), (12) or (13), (14).

In block j, the source splits the message d_j into m bitstreams according to $R_{CF}(k)$. $\{U_{k,\ell}^{(j)}:\ell\in Q_k\}$ carries bitstream at level k. $\{U_{k,\ell}^{(j)}:\ell\in Q_k^c\}$ are frozen to zero and revealed to the relay and the destination. Computing $\boldsymbol{u}_k^{(j)}G_2^{\otimes n}$ results in $\boldsymbol{a}_k^{(j)}$. Feeding $\boldsymbol{a}_k^{(j)}$ from all levels into the modulator generates the transmit signals $\boldsymbol{x}_1(d_j)$.

At the relay, based on $\mathbf{y}_{2}^{(j)}$, retrieved codewords of preceding levels $\{\tilde{\mathbf{a}}_{1}^{(j)} \cdots \tilde{\mathbf{a}}_{k-1}^{(j)}\}$ and frozen bits $\tilde{u}_{k,\ell}^{(j)} = u_{k,\ell}, \forall \ell \in Q_{k}^{c}$, an estimated $\{\tilde{u}_{k,\ell}^{(j)} : \ell \in Q_{k}\}$ is recovered successively as

$$\tilde{u}_{k,i} = \arg \max_{u \in \{0,1\}} p(u|\mathbf{y}_2^{(j)}, \tilde{\mathbf{a}}_1^{(j)} \cdots \tilde{\mathbf{a}}_{k-1}^{(j)}, \tilde{u}_{k,1}, \cdots, \tilde{u}_{k,i-1}).$$

Then, $\tilde{\boldsymbol{u}}_{k}^{(j)}$ is mapped to $\tilde{\boldsymbol{b}}_{k}^{(j)}$ via polar transform $G_{2}^{\otimes n}$. Feeding $\tilde{\boldsymbol{b}}_{k}^{(j)}$ from all levels into the modulator generates $\boldsymbol{x}_{2}(\tilde{d}_{j})$ which is transmitted in block j+1.

At the destination, based on $\mathbf{y}_{mrc}^{(j)}$, $\{\hat{\mathbf{a}}_{1}^{(j)}\cdots\hat{\mathbf{a}}_{k-1}^{(j)}\}$ and $\hat{u}_{k,\ell}^{(j)}=u_{k,\ell}, \forall \ell \in Q_{k}^{c}$, an estimated $\{\hat{u}_{k,\ell}^{(j)}: \ell \in Q_{k}\}$ is recovered successively as

$$\hat{u}_{k,i} = \arg \max_{u \in \{0,1\}} p(u|\mathbf{y}_{mrc}^{(j)}, \hat{a}_1^{(j)} \cdots \hat{a}_{k-1}^{(j)}, \hat{u}_{k,1}, \cdots, \hat{u}_{k,i-1}).$$

Finally \hat{d}_j is recovered by collecting $\{\hat{u}_{k,\ell}^{(j)}: \ell \in Q_k\}$ from all levels.

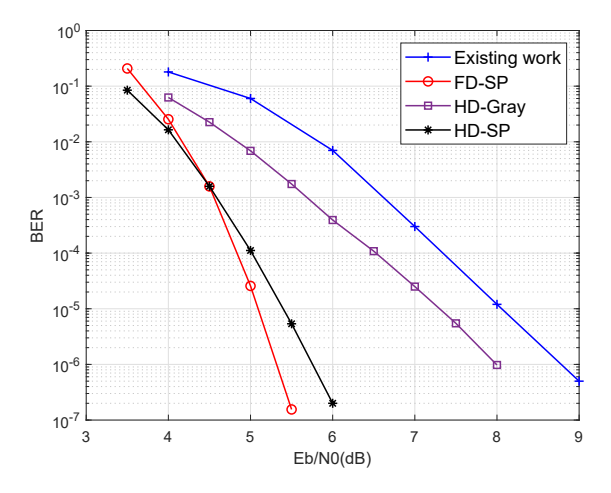
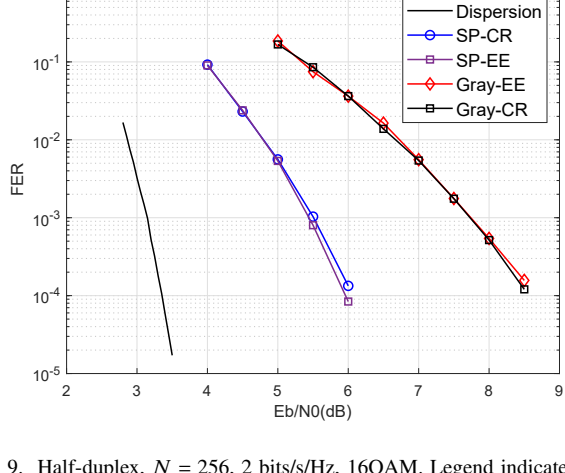


Fig. 7. N=1024, 2 bits/s/Hz, 16QAM, chain-rule based rate allocation. Legend indicates full-duplex (FD) vs. half-duplex (HD), and gray labeling (Gray) vs. Ungerboeck's set partitioning (SP).



100

Fig. 9. Half-duplex, N = 256, 2 bits/s/Hz, 16QAM. Legend indicates chainrule (CR) vs. error-exponent (EE) based rate allocations, and gray labeling (Gray) vs. Ungerboeck's set partitioning (SP).

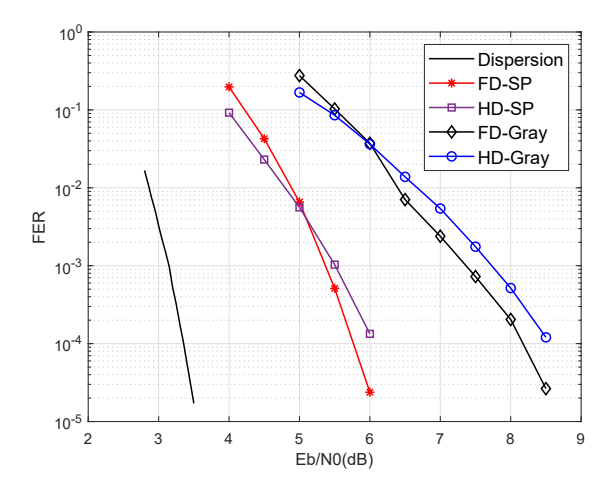


Fig. 8. N = 256, 2 bits/s/Hz, 16QAM, chain-rule based rate allocation. Legend indicates full-duplex (FD) vs. half-duplex (HD), and gray labeling (Gray) vs. Ungerboeck's set partitioning (SP).

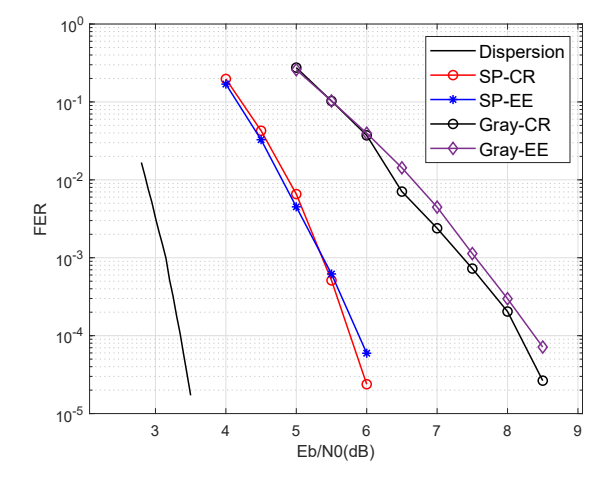


Fig. 10. Full-duplex, N = 256, 2 bits/s/Hz, 16QAM. Legend indicates chainrule (CR) vs. error-exponent (EE) based rate allocations, and gray labeling (Gray) vs. Ungerboeck's set partitioning (SP).

IV. SIMULATIONS

In this section, the simulation results for the decode-forward relaying with 16QAM are presented. The average power of source and relay is assumed to be equal throughout the experiments. We keep the channel coefficients $g_{13}=g_{12}=g_{23}=1$ and vary average source power (equivalently average relay power) to change SNRs of the decode-forward relay channel. The sum rate is $R_{DF}=2$ bits/s/Hz. Based on the rate allocations via chain rule in Figs. 3 and 4, the component polar codes have rates 0.62/0.38/0.62/0.38 bits/s/Hz and 0.04/0.35/0.65/0.96 bits/s/Hz for gray labeling and Ungerboeck's set partitioning respectively from the lowest level to the highest level. Using the rate allocations via error exponent in Figs. 5 and 6 generates rates 0.63/0.37/0.63/0.37 bits/s/Hz for gray labeling and 0.03/0.34/0.68/0.95 bits/s/Hz for Ungerboeck's set partitioning. In [13], the robust per-

formance of multi-level polar coded modulation using the construction in 5G standard [9] were shown. Therefore, we use the ordered indices available in 5G standard [9] to construct frozen and information sets. E_b/N_0 in the figures corresponds to the source-destination link. Block Markov coding with b=6 transmission blocks and forward decoding is applied in the full-duplex mode. The expectation and variance required in Equations (18) and (19) for computing the dispersion bounds are calculated by using Monte Carlo simulation.

In Fig. 7, we compare the proposed multi-level polar coded modulation in the BER performance with the existing work [7] where N = 1024 and the chain-rule based rates are used.

Any comparison between full-duplex and half-duplex relaying involves a subtlety that assumes more importance under short-block lengths. The closest work in the literature to the results of this paper appeared in [7], which is in orthogonal

half-duplex mode, while our work is reported in both half-duplex and full-duplex. For reporting/comparing half-duplex results, we can match the conditions of [7]. For reporting full-duplex results, we used equivalent overall code rates as [7] so that error curves against E_b/N_0 can be meaningfully compared. However, it is not possible to equalize *both* code rates and codeword block lengths in orthogonal half-duplex against full-duplex, therefore our full-duplex curves operate at block length 1024, while the half-duplex [7] operates at *end-to-end* block length 1024, which means the half-duplex relay and destination decode codewords that have length 512. A direct comparison in half-duplex mode shows 2.5dB gain at BER 10^{-5} for our method, while our full-duplex results compared with half-duplex results of [7] show a gain of 3dB at BER 10^{-6} .

The 2.5dB gain in the half-duplex mode over [7] can be explained as follows: 0.7dB gain comes from the multistage decoding, since [7] applied parallel independent decoding, which cannot benefit from the recovered codewords of preceding levels. The remaining 1.8dB gain is attributed to Ungerboeck's set partitioning. In [17], Ungerboeck's set partitioning has found to be effective in preventing error propagation when using multistage decoding. Together, these two factors explain the significant gain enjoyed by our method.

In Fig. 7, there is a cross-over of two BER curves which is deserving of an explanation. At low SNR, our full-duplex method performs worse than our half-duplex method; this is due to error propagation across message blocks in block Markov coding. At higher E_b/N_0 , error propagation is less prominent, so the full-duplex mode starts to outperform the half-duplex mode.

In order to investigate the performance using different labeling and rate allocations in both half-duplex and full-duplex short-block length regimes, we simulate the FERs for N=256 in Figs. 8-10. In Fig. 8 where the rate allocation follows the chain rule, Ungerboeck's set partitioning shows better performance than gray labeling in both half-duplex and full-duplex modes. In Figs. 9 and 10 where different rate allocation rules are used, the error exponent performs slightly better than the chain rule only at higher E_b/N_0 in the half-duplex mode with Ungerboeck's set partitioning in Fig. 9.

V. CONCLUSION

A decode-forward relaying using multi-level polar coded modulation is proposed. The chain rule and error exponent are used to determine the rates of polar codes. The joint decoding based on maximum ratio combining and multistage decoding is applied at the destination. We present the error performance in the half-duplex and full-duplex modes using different labeling and rate allocations. The simulation results show our method has a significant performance improvement over prior work.

REFERENCES

- G. Durisi, T. Koch, and P. Popovski, "Toward massive, ultrareliable, and low-latency wireless communication with short packets," *Proc. IEEE*, vol. 104, no. 9, pp. 1711–1726, 2016.
 A. A. Abotabl and A. Nosratinia, "Multilevel coded modulation for
- [2] A. A. Abotabl and A. Nosratinia, "Multilevel coded modulation for the full-duplex relay channel," *IEEE Trans. Wireless Commun.*, vol. 17, no. 6, pp. 3543–3555, 2018.
- [3] H. Wan, A. Høst-Madsen, and A. Nosratinia, "Compress-and-forward via multilevel coding," in *Proc. IEEE Int. Symp. on Info. Theory (ISIT)*, Jul. 2019, pp. 2024–2028.
- [4] H. Wan, A. Hxst-Madsen, and A. Nosratinia, "Compress-and-forward via multilevel coding and trellis coded quantization," *IEEE Commun. Lett.*, pp. 1–1, 2021.
- [5] R. Blasco-Serrano, R. Thobaben, M. Andersson, V. Rathi, and M. Skoglund, "Polar codes for cooperative relaying," *IEEE Trans. Commun.*, vol. 61, no. 2, pp. 3263–3273, Feb. 2015.
- [6] N. Madhusudhanan and L. Nithyanandan, "Compress-and-forward relaying with polar codes for LTE-A system," in *Int. Conf. Commun. and Signal Processing*, 2014, pp. 798–802.
- [7] X. Ma, L. Li, M. Zhu, W. Chen, and Z. Han, "Multilevel polar-coded modulation based on cooperative relaying," in *Proc. Int. Conf. Wireless Commun. and Signal Proc.*, 2017, pp. 1–4.
- [8] E. Arikan, "Channel polarization: A method for constructing capacity-achieving codes for symmetric binary-input memoryless channels," *IEEE Trans. Inf. Theory*, vol. 55, no. 7, pp. 3051–3073, 2009.
- [9] ETSI 3rd Generation Partnership Project (3GPP), Multiplexing and channel coding. Release 15, 3GPP Standard TS 38.212, Dec. 2019.
- [10] E. Arikan, "From sequential decoding to channel polarization and back again," available at https://arxiv.org/abs/1908.09594, Aug. 2019.
- [11] Y. Polyanskiy, H. V. Poor, and S. Verdu, "Channel coding rate in the finite blocklength regime," *IEEE Trans. Inf. Theory*, vol. 56, no. 5, pp. 2307–2359, 2010.
- [12] A. Elkelesh, M. Ebada, S. Cammerer, and S. ten Brink, "Belief propagation list decoding of polar codes," *IEEE Commun. Lett.*, vol. 22, no. 8, pp. 1536–1539, 2018.
- [13] J. Dai, J. Piao, and K. Niu, "Progressive rate-filling: A framework for agile construction of multilevel polar-coded modulation," *IEEE Wireless Commun. Lett.*, pp. 1–1, 2021.
- [14] L. Wang, "Polar coding for relay channels," in Proc. IEEE Int. Symp. on Info. Theory (ISIT), 2015, pp. 1532–1536.
- [15] A. El Gamal and Y.-H. Kim, Network Information Theory, 1st ed. Cambridge, U.K: Cambridge University Press, 2012.
- [16] G. Ungerboeck, "Channel coding with multilevel/phase signals," *IEEE Trans. Inf. Theory*, vol. 28, no. 1, pp. 55–67, Jan. 1982.
- [17] U. Wachsmann, R. F. H. Fischer, and J. B. Huber, "Multilevel codes: theoretical concepts and practical design rules," *IEEE Trans. Inf. Theory*, vol. 45, no. 5, pp. 1361–1391, 1999.
- [18] Y. Hu, J. Gross, and A. Schmeink, "On the capacity of relaying with finite blocklength," *IEEE Trans. Veh. Technol.*, vol. 65, no. 3, pp. 1790– 1794, 2016.
- [19] E. C. Song and G. Yue, "Finite blocklength analysis for coded modulation with applications to link adaptation," in *Proc. IEEE Wireless Commun. and Networking Conf.*, 2019, pp. 1–7.